Bioelectromagnetics 16:160–171 (1995)

Absorbed Energy Distribution From Radiofrequency Electromagnetic Radiation in a Mammalian Cell Model: Effect of Membrane-Bound Water

Li-Ming Liu and Stephen F. Cleary

Physiology Department, Medical College of Virginia, Virginia Commonwealth University, Richmond, Virginia

The spatial distributions of induced 27 or 2450 MHz radiofrequency (RF) electric fields (E-fields) and specific absorption rates (SARs) in a three-component spherical cell model (cytoplasm, membrane, extracellular space) were determined by Mie scattering theory. The results were compared to results for the same cell model but with 0.5 nm thick of bound water on the inner (cytoplasmic) and outer (extracellular) membrane surfaces (i.e., five-component cell model). The results provide insight regarding direct frequency-dependent RF radiation effects at the cellular level. Induced E-fields and SARs were calculated for two bound-water characteristic frequencies (400 or 1000 MHz) and ionic conductivities (1–1000 mS/m). In order to estimate the dependence of the results on bound water within the membrane per se, the model was revised to include bound water within the inner and outer membrane surfaces. The results were as follows: 1) On the x-axis, the y- and z-components of the induced E-field were of insignificant magnitude compared to the x-component for an incident E-field parallel to the x-axis; 2) the ratio of transmembrane E-fields induced by 2450 MHz vs. 27 MHz RF [i.e., E_x (2450 MHz)/E_x (27 MHz)] was 0.1; 3) for the three-component cell model, the corresponding SAR ratios [SAR (2450 MHz)/SAR (27 MHz)] in the cytoplasm and extracellular space were 1.66 and 5.0, respectively; 4) the SAR ratios [SAR (2450 MHz)/SAR (27 MHz)] for the cytoplasm and extracellular space for the five-component cell model were 1.66 and 5.0, respectively; 5) the ratio of the E-fields induced in the cytoplasmic and extracellular layers of bound water in the five-component cell model [E (2450 MHz)/E (27 MHz)] were 0.62 and 0.63, respectively; 6) the SAR ratios [SAR (2450 MHz)/SAR (27 MHz)] for the cytoplasmic and extracellular bound-water layers were 66 and 65.3, respectively; and 7) variation of bound-water characteristic frequency, ionic conductivity, or bound-water incorporation inside the membrane surfaces, per se, did not significantly affect the E-field or SAR ratios. These results indicate that frequency-dependent nonuniformities may occur in the distribution of induced RF E-fields and SARs at the cellular level.

Keywords: RF radiation, E-field, SAR, cell model, membrane, free water, bound water

INTRODUCTION

The results of an increasing number of studies indicate that radiofrequency (RF) electromagnetic radiation can directly affect living systems [Cleary, 1990a]. A variety of physiological alterations have been reported to occur under exposure conditions that do not involve detectable levels of heating. Documentation of direct or nonthermal RF exposure effects on humans or experimental animals involves inherent ambiguities due to 1) nonuniform RF absorption in tissue and the inability to adequately characterize such absorption distributions and 2) the complex interactive nature of mammalian organ systems. Results of in vitro studies of RF exposure effects on cells, conducted under controlled conditions, provide the most convincing evidence of direct RF exposure effects. However, the mechanisms for such effects remain uncertain [Cleary, 1990a,b].

The purpose of this study was to provide insight regarding the mechanisms of direct RF cellular effects. The approach taken was to calculate the electric field strength (E) and specific absorption rate (SAR) distributions in mammalian cell models. The general ratio-

Received for review December 28, 1992; revision received September 8, 1994.

Address reprint requests to Li-Ming Liu, Physiology Department, Box 980551, Medical College of Virginia, Richmond, VA 23298.

nale for this approach is based on the assumption that the most fundamental variable involved in direct RF-induced molecular alterations is the local electric field strength (E_l) or the directly related local SAR_l defined as

$$SAR_l = \sigma |E_l|^2 / \rho (W/kg) \quad (1)$$

where E_l is the root mean-square local electric-field strength, the effective conductivity (σ) is equal to the sum of the dielectric conductivity $\sigma_d = \omega\varepsilon''$ and the ionic conductivity σ_i (i.e., $\sigma = \sigma_d + \sigma_i$), and ρ is the density. An example of an E-field-dependent direct RF effect would be a field-induced biomolecular conformational alteration or dipole reorientation that did not occur as a result of an elevation in temperature of the localized molecular environment.

The true distinction between E-field-dependent vs. SAR-dependent alterations is somewhat arbitrary. In the present context, SAR-dependent effects are considered to be those due to alteration of the microenvironment of a target structure such as a cell-membrane receptor. This assumption relates to the fact that σ in Equation 1 is an extrinsic variable that reflects the averaged dielectric properties of the target microenvironment, which, in a living system, is primarily water. In this sense, therefore, E-field effects may be considered to be direct field effects on specific cell structures, whereas SAR-dependent effects involve the microenvironment of such structures. Because molecular level mechanisms for RF effects are not well understood, both variables were estimated.

Considering the frequency-dependent properties of biomolecules such as proteins and water, the relative contribution of direct E-field vs. localized SAR effects will depend on electromagnetic field frequency. The lowest frequency considered in this study (27 MHz) is higher than the relaxation frequency of protein molecules. Because the upper frequency (2450 MHz) is in the range of bound- and free-water relaxation, it may be speculated that bioeffects in this frequency range are more dependent on alteration of the aqueous microenvironment than on direct effects on biomolecules or biomolecular complexes. For the same reason, field-induced counter-ion relaxations, which occur at much lower frequencies, should not contribute significantly to RF effects considered here.

The choice of RF frequencies was based on previous studies of RF cellular effects and on the fact that the frequencies used in these calculations, namely, 27 MHz and 2450 MHz, are the RF frequencies to which human beings are most frequently exposed in the home and in the workplace. Exposure of normal human peripheral lymphocytes to 27 or 2450 MHz continuous-wave (CW) or pulse-modulated (PM) RF radiation under isothermal (37 ± 0.2 °C) conditions using an SAR range of 0.5–200 W/kg resulted in biphasic modulation of cell proliferation rate [Cleary et al., 1990a, 1992]. A similar modulation of cell proliferation occurred when glioma cells, a transformed cell line, were exposed under the same conditions [Cleary et al., 1990b, 1992]. Based on the known frequency-dependent dielectric properties of cell membranes at these frequencies, Cleary et al. [1990b] noted that 27 MHz RF radiation would induce a transmembrane potential approximately ten times greater than 2450 MHz radiation. It should be noted, however, that, at RF intensities to which living systems are normally exposed, the field-induced potentials are many orders of magnitude lower than cell-membrane resting potentials. Whereas 2450 MHz radiation had a greater effect on lymphocyte or glioma proliferation than 27 MHz, the response was not proportional to the magnitude of the induced transmembrane potentials. This suggested the possibility that a factor (or factors) other than RF-induced transmembrane potential was more directly responsible for effects on cell proliferation, and it indicated the need for more detailed knowledge of cellular-level distributions of RF-induced fields.

This paper considers the effect of absorption of 27 and 2450 MHz RF radiation in bound (vicinal) water vs. free (unbound) water in a mammalian cell model. Although detailed information on the exact amount and distribution of cellular bound water is limited, it is well known that all lipid bilayers, including biomembranes, have associated layers of bound water. It was determined experimentally that bound-water dielectric relaxation occurs at significantly lower RF frequencies than free-water dielectric relaxation. Based on studies of dielectric properties of protein-bound water [Grant et al., 1974, 1978], a bound-water relaxation (characteristic) frequency f_c^b of 400 MHz was predicted. Free-water relaxation occurs in the range of 10–100 GHz, depending on temperature. Differences in dielectric relaxation frequencies and the nonuniform spatial distribution of cellular free vs. bound water suggest frequency-dependent differences in the distribution of absorbed RF electromagnetic energy in cells. The calculations summarized here indicate the relative magnitudes of the induced transmembrane potentials and SARs in the vicinity of a cell membrane with or without a two-molecule-thick layer of bound water on the inner and outer surfaces of the cell plasma membrane.

CELL MODEL

The cell model was a sphere with a 3.5 μm radius (r_1) surrounded by a bilayer lipid membrane with a thickness (d) of 10 nm. The cytoplasm was modelled as physi-

ological saline (0.07 N) containing a protein volume fraction of 0.262 [Drago and Ridella, 1982]. Cytoplasmic protein had 0.28 g bound water per gram of protein; the remainder of the cytoplasmic water was assumed to be free water. The characteristic frequency of protein dielectric relaxation was 2 MHz, which was based on the results of Schwan [1977] and Grant et al. [1978]. The static (ε'_s) and high-frequency (ε') relative permitivities of protein were 380 and 2.0, respectively [Schwan, 1977; Grant et al., 1978]. The cell was suspended at infinite dilution in an extracellular medium that consisted of electrolytes in free water; the medium was assumed to have the frequency-dependent dielectric properties of physiological saline. For the first series of calculations summarized here, the membrane consisted of a phospholipid bilayer that had a frequency-independent relative permitivity (ε') of 11.3 (membrane capacity, 1.0 μF/cm^2) and 0 ($\sigma = 0$) conductivity [Schwan, 1971].

The effect of cellular bound water on the spatial distribution of the E-field and SAR induced by RF electromagnetic radiation absorption was determined by comparing the results of calculations using a simple, three-component spherical cell model with a plasma membrane to calculations using a five-component spherical model with a plasma membrane and with a 0.5 nm layer of bound water on the inner (cytoplasmic) and outer (extracellular) surfaces. Figure 1 indicates the three-component cell model in a lossy medium that was exposed to a plane electromagnetic wave with a propagation vector (k) parallel to the z-axis of the sphere and with E- and B-field components parallel to the x- and y-axis, respectively.

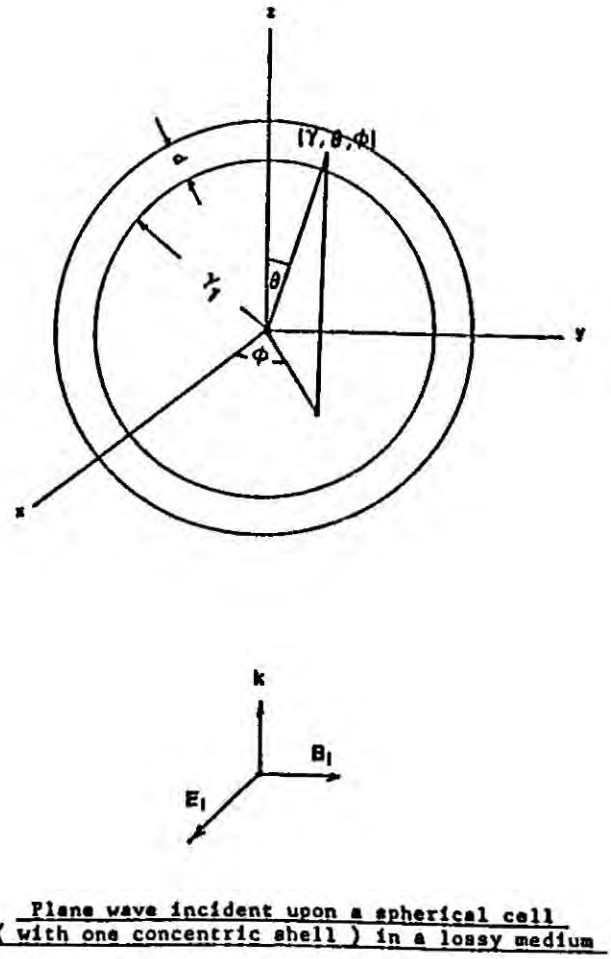

Fig. 1. Spherical model of a mammalian cell with a concentric shell (cell membrane) in a lossy dielectric medium (cell culture medium) exposed to a plane radiofrequency electromagnetic wave with propagation vector $\bar{k}$ parallel to the +z-axis, E-field parallel to the +x-axis, and $\bar{B}$-field parallel to the +y-axis.

DIELECTRIC PARAMETERS

The relative permitivity (ε') and the dielectric conductivity $\sigma_d = \omega\varepsilon''$ (where ω is the angular frequency of the electromagnetic field, and ε'' is the imaginary part of the complex dielectric constant ε^*) were obtained from Drago and Ridella [1982] and Jaroszyński et al. [1983]. The dielectric values that were used to calculate induced E-fields and SAR distributions in the three- and five-component cell models exposed to 27 or 2450 MHz plane-wave electromagnetic fields are summarized in Table 1. The static (ε_s) and high frequency (ε_∞) relative permitivities of free and bound water were 80.0 and 4.9, respectively [Grant et al., 1978]. The frequency dispersion of bound water occurs in the range of 200–1000 MHz [Cook and Kuntz, 1974]. Depending on the distance from macromolecular or membrane surfaces, there is more than one relaxation time for bound water associated with biological systems in these frequency ranges [Colonomos and Gordon, 1979; Foster et al., 1984]. We chose two relaxation frequencies at either end of the relaxation spectrum, namely, 400 [Grant et al., 1978] and 1000 MHz, in order to determine how the value of this parameter affected E-field and SAR ratios at 27 and 2450 MHz. Again, due to uncertainty about the true ionic conductivity of membrane-bound water, (σ_i^b), we selected ionic conductivities of 1 mS/m or 1 S/m, which correspond to dilute protein solutions or biological fluids in vivo, respectively [Dawkins et al., 1979]. The corresponding dielectric conductivities or dielectric constants were determined by the Debye relationship (σ_d^b). The characteristic relaxation frequency of free water (f_c^f) was assumed to be 20 GHz [Schwan, 1977].

Figure 2 shows schematic cross sections of the three-, five-, and seven-component spherical cell models that indicate the location of the extramembranous layers of bound water (five-component model). The

TABLE 1. Dielectric Parameters for Cell Model Calculations*

	27 MHz		2450 MHz	
Model Component	ε'	σ^a (s/M)	ε'	σ^a (s/M)
Cytoplasm	57.145[b]/56.216[c]	0.6004[b]/0.6880[c]	48.677[b]/48.699[c]	1.3237[b]/1.4172[c]
Cell membrane	11.3	—	11.3	—
Bound water[b]	79.66	0.00864[b]/1.0076[c]	6.851.6265[b]/2.6256[c]	
Bound water/membrane[d]	11.984	$8.64 \times 10^{-5(b)}/1.0076 \times 10^{-2(c)}$	11.256	$1.6265 \times 10^{-2(b)}/2.6256 \times 10^{-2(c)}$
Extracellular medium	71.465	1.928	70.87	2.781

*Cell radius, 3.5 μm; thickness of membrane-bound waters, 1.0 nm; depth of penetration of intramembrane-bound water, 0.5 nm; membrane bound-water relaxation frequency, 400 MHz.
[a]Effective conductivity (dielectric + ionic; S/m).
[b]Bound-water ionic conductivity, 1 mS/m.
[c]Bound-water ionic conductivity, 1 S/m.
[d]One volume % solution of bound water incorporated into a 0.5-nm-thick membrane surface layer.

seven-component model also includes regions of bound water incorporated into the cytoplasmic and extracellular membrane surface, per se.

SOLUTION

The spatial distribution of the E-field induced in the spherical cell model with and without membrane bound-water layers was determined by using the Mie scattering theory [formulated by Stratton, 1941]. The theory permitted determination of the E-field components $E(r,\Theta,\phi)$ by expanding the incident, scattered, and induced E- and B-field components of the RF electromagnetic field into vector-spherical harmonics.

Because the dimensions of the cell model were small in comparison to the RF wavelengths, an alternative to the Mie theory solution would have been a quasistatic approximation involving solution of the 0th-order field using Laplace's equation and the 1st-order field with perturbation theory [Van Bladel, 1985]. We chose the

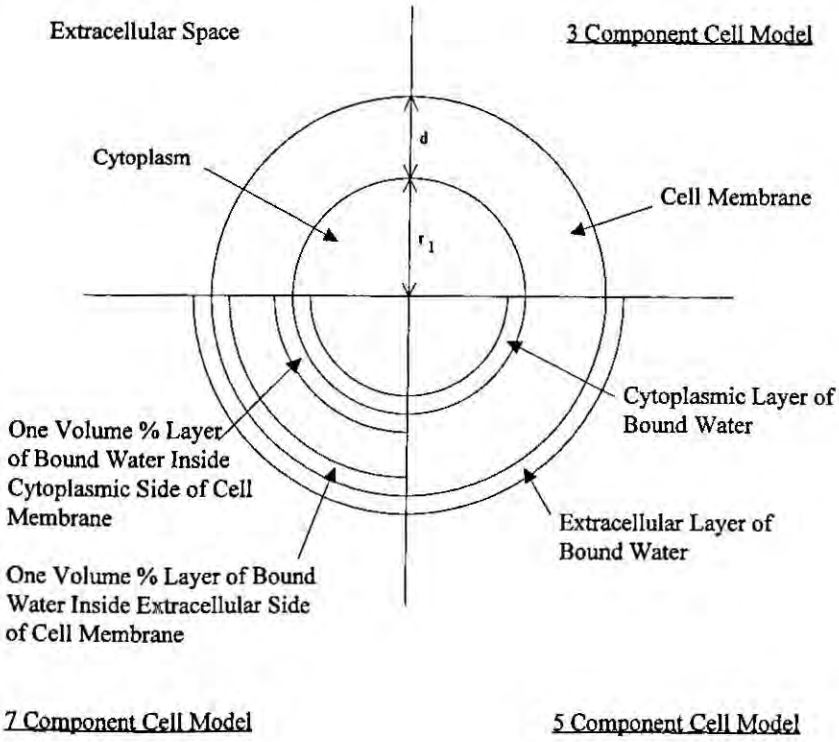

Fig. 2. Schematic cross sections of the three-, five-, and seven-component spherical cell models indicating the location of the extramembranous layer of bound water (five-component model) and the bound-water layers incorporated into the cytoplasmic and extracellular membrane surfaces, *per se*, in the seven-component cell model (see text for details).

Mie theory solution, because it is applicable to dielectric spheres of a wider size range and, thus, it is more generally useful.

For any region(s) of the three- or five-component spherical cell model, the solutions for the E- and B-field components are given by the expressions:

$$E_s = E_0 \sum_{n=1}^{\infty} i^n \frac{(2n+1)}{n(n+1)}\left[a_{ns} M_{o1n}^{(1)} - ib_{ns} N_{e1n}^{(1)} + C_{ns} M_{o1n}^{(3)} - id_{ns} N_{e1n}^{(3)}\right] \quad (2)$$

$$B_s = -\frac{k_s}{\omega} E_0 \sum_{n=1}^{\infty} i^n \frac{(2n+1)}{n(n+1)}\left[b_{ns} M_{e1n}^{(1)} + ia_{ns} N_{o1n}^{(1)} + d_{ns} M_{e1n}^{(3)} + ic_{ns} N_{o1n}^{(3)}\right] \quad (3)$$

where **M** and **N** are vector-spherical harmonics that are dependent on radiation frequency and frequency-dependent dielectric properties. The constants a_{ns}, b_{ns}, c_{ns}, and d_{ns} are determined by the boundary conditions:

$$(E_s)_\theta = (E_{s+1})_\theta \qquad (B_s)_\theta = (B_{s+1})_\theta$$

$$(E_s)_\phi = (E_{s+1})_\phi \qquad (B_s)_\phi = (B_{s+1})_\phi$$

(assuming $\mu = \mu_0$). (4)

For s equal to 1 [inner sphere (cytoplasm)], only spherical Bessel functions of the first kind are permitted (i.e., $c_{n,1} = d_{n,1} = 0$), and, for s equal to N (extracellular space), $a_{nN} = b_{nN} = 1$ at distances $r >> r_1 + d$, where the scattered field is 0.

A VAX mainframe computer employing double-precision arithmetic was used for the calculations. The number of terms included in the series expansion of Equations 2 and 3 were determined to satisfy the criteria:

$$|a_{ns}|^2 + |b_{ns}|^2 \leq 10^{-14}.$$

The validity of the Mie theory in this application was determined by comparing these results to the results of a closed-form quasistatic solution for the three-component cell model. The two methods agreed to within 0.00003%.

RESULTS

The induced fields [$E(r,\Theta,\phi)$] and localized SARs [$SAR(r,\Theta,\phi)$] were calculated in all regions of the cell models. The results summarized here are the maximum induced E-field components at points along the x-axis (E_{xmax}, E_{ymax}, E_{zmax}) and the maximum value of the SAR (SAR_{max}) for a 27 or 2450 MHz plane-wave electromagnetic field with an incident E-field strength of 1 V/m. The maximum induced transmembrane field strength on the x-axis for the field orientation shown in Figure 1 (i.e., $\mathbf{k} \| z$) corresponds to $E(r,\Theta,\phi) = E(r_1 + d, \pi/2, 0)$, which is denoted as E_{xmax} in the membrane region. The tangential E-field component for this orientation, $E(r,\Theta,\phi) = E(r_1 + d, \pi/2, \pi/2)$, is equal to E_{xmax} in the membrane region on the y-axis, whereas $E(r_1 + d, 0, 0)$ corresponds to E_{xmax} on the z-axis. Maximum values of the induced E-field components and SARs on the x-axis for the three-component and five-component (membrane-bound water) models are summarized in Tables 2 and 3 and are illustrated in Figures 3 and 4. For the sake of comparison, the magnitudes of E-fields and SARs on the y-axis are summarized in Table 4. The E-field components and SARs on the z-axis were also calculated, but the results are not summarized, because the results were similar to values for the y-axis.

The bound-water characteristic frequency (400 MHz) and ionic conductivity (1 mS/m) that were used in these calculations were obtained from the literature, as indicated above. Because these values were derived primarily from measurements of protein-bound water, it is possible that the values of these parameters may differ for membrane-bound water. In the absence of data with which to directly determine the accuracy of f_c^b and σ_i^b, we decided to estimate the relative sensitivity of the model calculations to variations in the value of these parameters.

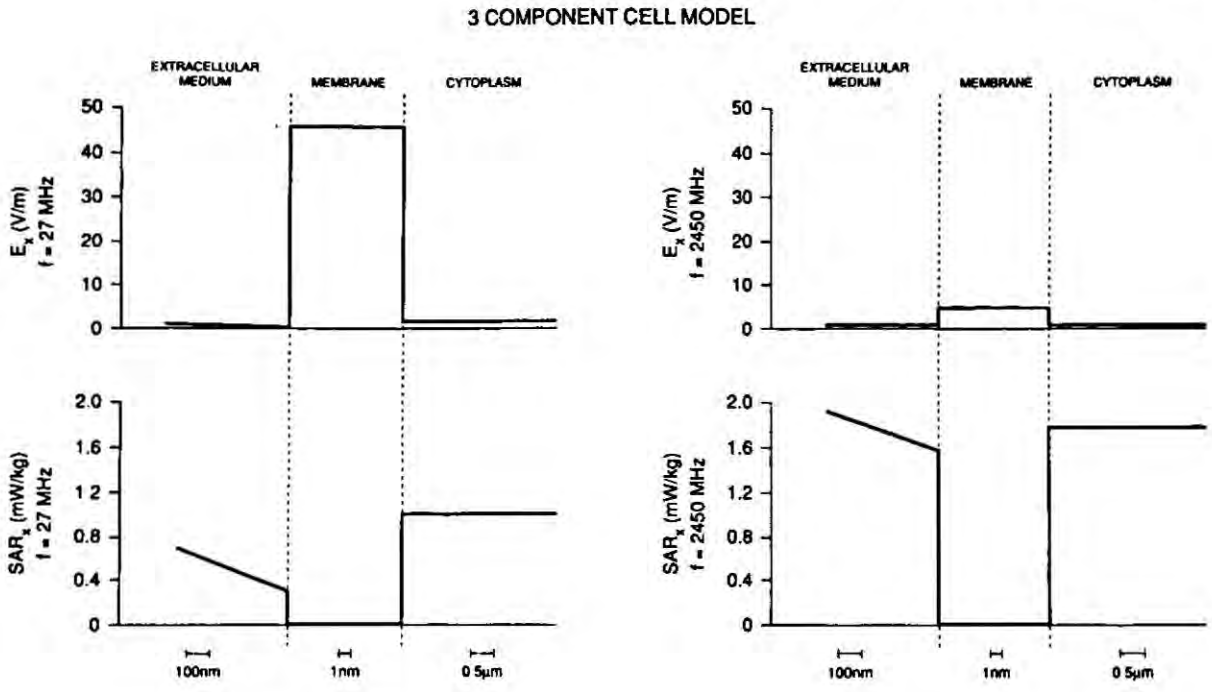

Fig. 3. Spatial distribution of the maximum induced E-field component (E_x) and specific absorption rate (SAR_x) on the x-axis of a three-component mammalian cell model (extracellular medium, cell membrane, cytoplasm) exposed to 27 or 2450 MHz continuous plane-wave electromagnetic radiation. Incident E-field strength, 1 V/m. Propagation vector orientation is shown in Figure 1.

RF field-induced maximum E-fields and SARs were calculated along the x-axis of a five-component cell model using the parameters that are listed in Table 3 with the exception of f_c^b, which was assumed to be equal to 1000 MHz; results are summarized in Table 5. The sensitivity of the model to the value of the ionic conductivity of bound water was tested using the same parameter values used in the five-component model (results summarized in Table 3) but using a value of the bound-water ionic conductivity σ_i^b of 1 S/m (i.e., an increase of three orders of magnitude). The results of these calculations are summarized in Table 6.

In order to estimate the dependence of the results on the assumed distribution of membrane-associated bound water, the model was revised by incorporating bound water into the inner and outer surfaces, per se, in addition to the extramembrane layers of bound water. Studies of the distribution of bound water in phospholipid bilayer membranes have indicated that water penetrates into the lipid head group regions of the membrane [McIntosh et al., 1989]. Griffith et al. [1974], for example, with the use of electron-spin resonance, estimated that water penetrates approximately one-third of the distance from each surface into microsomal and myelin membranes. In order to determine the sensitivity of the RF field-induced E-fields and SARs to water penetration into the membrane, calculations were made using the seven-component model shown in Figure 2. The seven-component model was identical to the five-component model (results summarized in Table 3) except for the inclusion of a 0.5-nm-thick area (approximate water-molecule diameter) in the inner (cytoplasmic) and outer (extracellular) membrane regions. The composition of these membrane layers was assumed to be a 1% solution of bound water in phospholipid. The dielectric constants for these membrane/bound-water regions are indicated in Table 1. The maximum RF-induced E-fields and SARs for this seven-layer model are also summarized in Table 7.

DISCUSSION

In view of uncertainties regarding the magnitudes of the relevant microscopic dielectric properties on the spatial scale that was used in these calculations, it was considered to be more logical to focus on relative, rather than absolute, values of cellular-level induced E-fields and SARs. Consequently, whereas induced field magnitudes are indicated in the Tables and in Figures 3 and 4, relative values (ratios) will generally be referred to

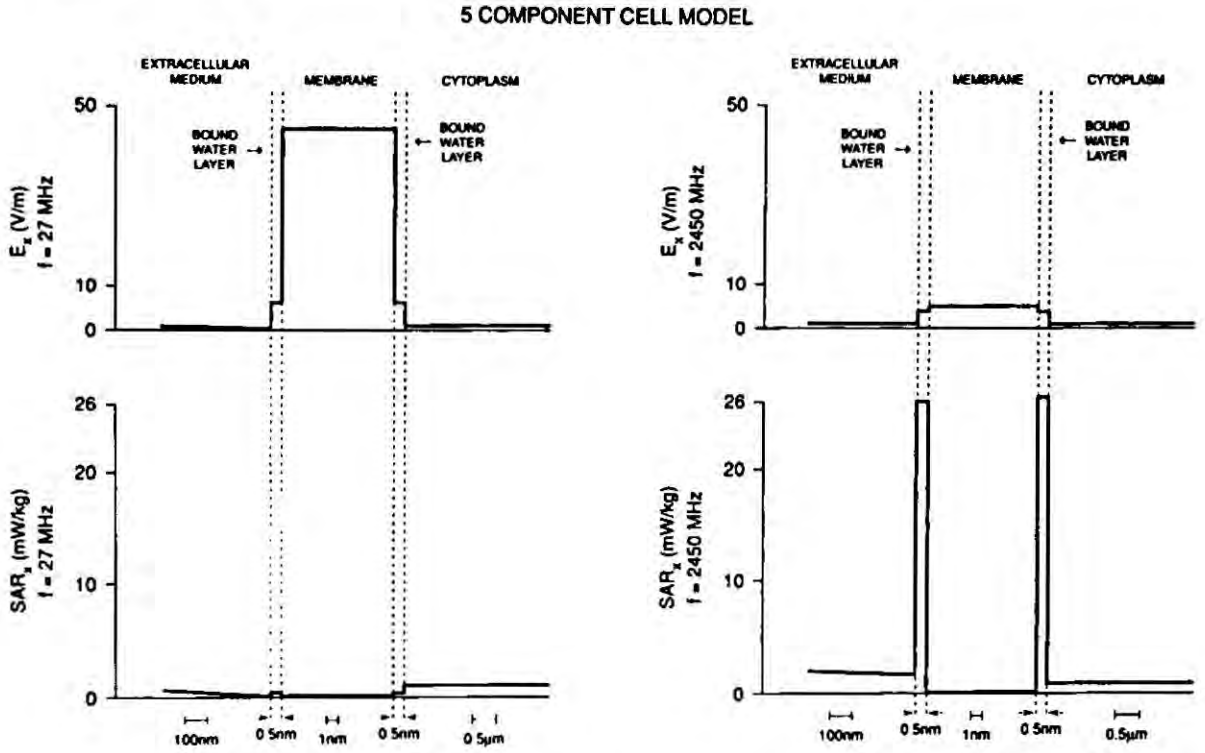

Fig. 4. Spatial distribution of the maximum induced E-field component (E_x) and SAR (SAR_x) on the x-axis of a five-component mammalian cell model (extracellular medium, bound-water layer on exterior cell membrane surface, cell membrane, bound-water layer on inside surface of cell membrane surface, cytoplasm) exposed to 27 or 2450 MHz continuous plane-wave electromagnetic radiation. Incident E-field strength, 1 V/m. Propagation vector orientation is shown in Figure 1.

in this discussion. These calculations were undertaken in order to provide insight regarding the interaction of RF radiation frequency and cell-bound water rather than to explain specific experimental results. This provides an additional rationale for considering relative, rather than absolute, values of induced fields. Whereas the results of these calculations cannot be verified experimentally due to spatial resolution limitations, further refinements and applications of models of this kind will permit predictions of the relationship between cell-level induced fields and specific cell physiologic alterations. For example, the results discussed below indicate that the SAR, which was calculated with cell membrane-associated bound water, is frequency dependent. The frequency dependence of specific cell physiologic endpoints, such as cation transport, can be measured experimentally in order to determine dependence on membrane bound-water SAR as a test of model predictions.

RF Frequency

The potential effects of RF-frequency and membrane-bound water may be compared using the results

TABLE 2. Maximum E-Fields and SAR Distribution Along X-Axis: Three-Component Model*

	Frequency							
	27.12 MHz				2450 MHz			
Region	E_{xmax} (V/m)	E_{ymax} (V/m)	E_{zmax} (V/m)	SAR (W/kg)	E_{xmax} (V/m)	E_{ymax} (V/m)	E_{zmax} (V/m)	SAR_{max} (W/kg)
Cytoplasm	1.28	0	1.35×10^{-5}	0.984	1.1	0	1.09×10^{-4}	1.64
Membrane	45.6	0	1.43×10^{-5}	0	4.9	0	1.26×10^{-4}	0
Medium adjacent to membrane	0.4	0	1.43×10^{-5}	0.31	0.75	0	1.26×10^{-4}	1.56

*Incident E-field, 1 V/m; SAR, specific absorption rate.

TABLE 3. Maximum E-Fields and SAR Distribution Along X-Axis: Five-Component Model*

	Frequency							
	27.12 MHz				2450 MHz			
Region	E_{xmax} (V/m)	E_{ymax} (V/m)	E_{zmax} (V/m)	SAR (W/kg)	E_{xmax} (V/m)	E_{ymax} (V/m)	E_{zmax} (V/m)	SAR_{max} (W/kg)
Cytoplasm	1.3	0	1.35×10^{-5}	1.0	1.1	0	1.09×10^{-4}	1.7
Cytoplasmic bound water[a]	6.5	0	1.35×10^{-5}	0.4	4.0	0	1.09×10^{-4}	26.3
Membrane	45.6	0	1.43×10^{-5}	0	4.9	0	1.30×10^{-4}	0
Extracellular bound water	6.4	0	1.43×10^{-5}	0.4	4.0	0	1.30×10^{-4}	26.1
Medium adjacent to extracellular bound water	0.4	0	1.43×10^{-5}	0.3	0.75	0	1.30×10^{-4}	1.6

*Incident E-field, 1 V/m; f_c^b = 400 MHz, σ_i^b = 1 mS/m.
[a]Effective conductivity of bound water, 8.64 mS/m (27 MHz) and 1.6266 S/m (2450 MHz).

for a three-component model (summarized in Table 2) to the results for a five-component cell model (summarized in Table 3) or by reference to Figures 3 and 4. The data shown in Table 2 indicate the following: 1) For the cell-RF field orientation that was assumed in these calculations (Fig. 1), the y and z E-field components were of insignificant magnitude relative to E_{xmax} on the x-axis; 2) the ratio of the magnitudes of transmembrane E-field strengths induced by 2450 MHz vs. 27 MHz RF radiation [i.e., E_{xmax} (2450 MHz)/E_{xmax} (27 MHz)] was 0.11; 3) SAR ratios for these RF frequencies [i.e., SAR (2450 MHz)/SAR (27 MHz)] in the cytoplasm and the extracellular space were 1.66 and 5.0, respectively. The three-component model predicted a significantly higher induced transmembrane potential at 27 MHz than at 2450 MHz because of the higher membrane impedance at the lower frequency. The lower membrane impedance and higher dielectric conductivity at 2450 MHz, when compared to 27 MHz, resulted in the indicated relative increases in SAR in the cytoplasm and extracellular space at the higher RF frequency. The physiological relevance of these results is uncertain. It could be argued that SAR-dependent effects in the cytoplasm, such as effects on cell organelles or the nucleus, would be more likely to occur as a result of exposure to 2450 MHz compared to 27 MHz. However, such SAR-dependent cellular responses have not been documented. Because the difference in cytoplasmic SARs at these frequencies is only about 66%, these results are of uncertain significance.

Bound Water

Comparing the field strength and SAR ratios for the five-component model in Table 3 to the ratios obtained for the three-component cell model in Table 2,

TABLE 4. Maximum E-Fields and SAR Distribution Along Y-Axis: Five-Component Model*

	Frequency							
	27.12 MHz				2450 MHz			
Region	E_{xmax} (V/m)	E_{ymax} (V/m)	E_{zmax} (V/m)	SAR (W/kg)	E_{xmax} (V/m)	E_{ymax}	E_{zmax}	SAR (W/kg)
Cytoplasm	1.28	0	0	1.0	1.12	0	0	1.65
Cytoplasmic bound water[a]	1.28	0	0	0.01	1.12	0	0	2.02
Membrane	1.30	0	0	0	1.11	0	0	0
Extracellular bound water	1.30	0	0	0.02	1.11	0	0	2.06
Medium adjacent to extracellular bound water	1.30	0	0	3.3	1.11	0	0	3.53

*Incident E-field, 1 V/m; f_c^b = 400 MHz; σ_i^b = 1 mS/m.
[a]Effective conductivity of bound water, 8.64 mS/m (27 MHz) and 1.6266 S/m (2450 MHz).

TABLE 5. Maximum E-Fields and SAR Distribution Along X-Axis: Five-Component Model*

	Frequency							
	27.12 MHz				2450 MHz			
Region	E_{xmax} (V/m)	E_{ymax} (V/m)	E_{zmax} (V/m)	SAR (W/kg)	E_{xmax} (V/m)	E_{ymax} (V/m)	E_{zmax} (V/m)	SAR (W/kg)
Cytoplasm	1.28	0	1.36×10^{-5}	1.0	1.12	0	1.07×10^{-4}	1.76
Cytoplasmic bound water*	6.45	0	1.36×10^{-5}	0.2	1.82	0	1.07×10^{-4}	11.8
Membrane	45.65	0	1.35×10^{-5}	0	4.91	0	1.25×10^{-4}	0
Extracellular bound water	6.41	0	1.43×10^{-5}	0.17	1.81	0	1.25×10^{-4}	11.7
Medium adjacent to extracellular bound water	0.40	0	1.43×10^{-5}	0.31	0.75	0	1.25×10^{-4}	1.56

*Incident E-field, 1 V/m; f_c^b = 1000 MHz; σ_i^b = 1 mS/m.
*Effective conductivity of bound water, 4.1 mS/m (27 MHz) and 3.577 S/m (2450 MHz).

it may be concluded that the presence of cytoplasmic and extracellular layers of membrane-bound water had minimal effects on induced transmembrane potentials or on cytoplasmic and extracellular SAR at 27 or 2450 MHz. The ratio of the E-fields induced in the cytoplasmic and extracellular layers of bound water at these frequencies [E(2450 MHz)/E(27 MHz)] were 0.62 and 0.63, respectively.

The SAR ratios [SAR(2450 MHz)/SAR(27 MHz)] for the cytoplasmic- and extracellular bound-water layers were 65.8 and 65.3, respectively. Thus, for these RF frequencies, the inclusion of membrane bound-water layers introduced significant frequency-dependent nonuniformities in SAR distributions in the immediate vicinity of the cell membrane. The relative magnitude of the SAR ratios was directly attributed to the higher effective conductivity at 2450 MHz compared to 27 MHz (1.6256 S/m and 8.64 mS/m, respectively). These results indicate that SAR-dependent cellular alterations would predominate at RF frequencies in the range of bound-water relaxation relative to the effects of lower frequency radiation.

Incident E-field Orientation

The maximum E-field and SAR components along the y-axis of the five-component cell model are summarized in Table 4. Comparing these results to the values obtained on the x-axis of the cell model, the following may be concluded: 1) Induced E-fields and SARs on the y-axis for both RF frequencies are lower than on the x-axis except in the extracellular compartment, where the E-fields were approximately three times greater along the y-axis than along the x-axis at 27 MHz and were about 1.4 times greater at 2450 MHz. 2) At 27 MHz, the ra-

TABLE 6. Maximum E-Fields and SAR Distribution Along X-Axis: Five-Component Model*

	Frequency							
	27.12 MHz				2450 MHz			
Region	E_{xmax} (V/m)	E_{ymax} (V/m)	E_{zmax} (V/m)	SAR (W/kg)	E_{xmax} (V/m)	E_{ymax} (V/m)	E_{zmax} (V/m)	SAR (W/kg)
Cytoplasm	1.26	0	1.28×10^{-5}	1.09	1.12	0	1.07×10^{-4}	1.76
Cytoplasmic bound water*	0.86	0	1.28×10^{-5}	0.74	2.71	0	1.07×10^{-4}	19.3
Membrane	51.16	0	1.33×10^{-5}	0	4.91	0	1.25×10^{-4}	0
Extracellular bound water	0.85	0	1.33×10^{-5}	0.73	2.70	0	1.25×10^{-4}	19.15
Medium adjacent to extracellular bound water	0.45	0	1.33×10^{-5}	0.39	0.75	0	1.25×10^{-4}	1.56

*f_c^b = 400 MHz; σ_i^b = 1 S/m.
*Effective conductivity of bound water, 1.0076 S/m (27 MHz) and 2.6256 S/m (2450 MHz).

tio of SAR in the extracellular space at the y-axis pole to the x-axis pole was 11, whereas this ratio was 2.2 at 2450 MHz. Thus, the y-axis tangential induced E-field (i.e., the maximum E-field on the y-axis) in the extracellular space resulted in an enhancement in SAR relative to SARs in other components. However, the enhancement was significantly less than the enhancement in SAR in the membrane bound-water layers that occurred at the x-axis pole at 2450 MHz. The x-component of the tangential E-field strengths (for the RF field polarity shown in Fig. 1) was approximately equal to the incident field strength. Thus, SAR at the extracellular surface depended on the local conductivity.

Bound-Water Relaxation Frequency

It should be noted that this cell model is highly simplified, because it does not take into account geometrical variations (e.g., nonspherical cells), cell surface irregularities, dynamic properties of cell membranes, or spatial variation in the dielectric properties of cell membrane-associated water. Calculations were made assuming a layer of bound water associated with a spherical membrane surface in contact with either extracellular or cytoplasmic free water. A more realistic model would consist of membrane-associated water with varying dielectric properties (e.g., characteristic frequency) between bound water at the membrane surface and free water in the surrounding extracellular medium. Theoretical studies involving more detailed cell models will be the object of future calculations, pending the availability of requisite data pertinent to the local field problem at the cell membrane surface.

Whereas a simplified approach was taken in this paper, an attempt was made to determine the sensitivity of the results to modelling uncertainties. In order to obtain insight regarding the relationship of bound-water characteristic relaxation frequency (f_b^c) and RF-induced E-fields and SARs, calculations were made using the five-component model but assuming f_c^b = 1000 MHz instead of 400 MHz, which was the value used in the calculations summarized in Table 3. The value of f_c^b = 1000 MHz was chosen to test the relative sensitivity of the model to this parameter value. This value of f_c^b was in the range between the reported bound-and free-water characteristic relaxations of 400 MHz and 20,000 MHz, respectively. Because there is a transition in the state of cell membrane-associated water from the fully bound to the free state, due to spatial variation in the average number of hydrogen bonds per water molecule, it was assumed that intermediate values of f_c^b were appropriate in certain regions in the vicinity of cell membranes.

The results of assuming f_c^b = 1000 MHz in calculations of induced fields and SARs in the five-component cell model are summarized in Table 5. In comparing these results to those of Table 3, it is apparent that, in general, the results were relatively insensitive to the value of f_c^b. The most obvious effect of selecting a higher value of f_c^b was an approximate twofold reduction in the estimated SAR in the bound-

TABLE 7. Maximum E-Fields and SAR Distribution Along X-Axis: Seven-Component Model*

	Frequency							
	27.12 MHz				2450 MHz			
Region	E_{xmax} (V/m)	E_{ymax} (V/m)	E_{zmax} (V/m)	SAR (W/kg)	E_{xmax} (V/m)	E_{ymax} (V/m)	E_{zmax} (V/m)	SAR (W/kg)
Cytoplasm	1.28	0	1.36×10^{-5}	0.99	1.12	0	1.07×10^{-4}	1.65
Cytoplasmic bound water	6.5	0	1.36×10^{-5}	0.36	2.71	0	1.07×10^{-4}	26.32
Bound water in cytoplasmic membrane surface	43.0	0	1.35×10^{-5}	0.16	4.93	0	1.08×10^{-4}	0.39
Membrane	45.6	0	1.41×10^{-5}	0	4.90	0	1.24×10^{-4}	0
Bound water in extracellular membrane surface	42.8	0	1.43×10^{-5}	0.16	4.91	0	1.25×10^{-4}	0.39
Extracellular bound water	6.4	0	1.43×10^{-5}	0.36	2.70	0	1.25×10^{-4}	26.0
Medium adjacent to extracellular bound water	0.4	0	1.43×10^{-5}	0.31	0.75	0	1.25×10^{-4}	1.55

*f_c^b = 400 MHz; σ_i^b = 1 mS/m.

water layers. Because the bound-water layer SARs were reduced by approximately the same factor at 27 and 2450 MHz, the SAR ratios at these frequencies remained about the same as those shown in Table 2, where it was assumed that $f_c^b = 400$ MHz. It should be noted that this conclusion regarding the effect of f_c^b pertains to the RF frequencies used in these calculations (viz. 27 and 2450 MHz) and is not true in general.

Bound-Water Conductivity

Uncertainty about the value of ionic conductivity (σ_i^b) in cell membrane-bound water suggested the need to perform the calculations summarized in Table 6. These calculations were performed using the same five-component cell model and parametric values as in Table 3 but assuming $\sigma_i^b = 1$ S/m. This value of ionic conductivity was considered to be an extreme upper limit, because it is approximately equal to that of a typical biological fluid in vivo. Therefore, most likely, it is a significant overestimate of the true bound-water conductivity. In comparing the results summarized in Tables 2 and 6, however, it was apparent that the RF-induced SARs were not affected significantly by an increase of three orders of magnitude in σ_i^b. The decreased impedance of the bound-water layers resulted in a decrease of approximately one order of magnitude in the E-fields induced across the bound-water layer at 27 MHz. There was an approximate 30% decrease in the E-fields induced in the bound-water layers at 2450 MHz.

Membrane-Incorporated Bound Water

Detailed quantitative information about the dielectric properties and distribution of cell water at the scale of these calculations is lacking, as previously noted. Reports indicate that bilayer phospholipid membrane head group regions may include a relatively small but detectable fraction of bound water [Griffith et al., 1974]. The calculations using a seven-component spherical cell model (summarized in Table 7) were performed in order to estimate how the inclusion of 1% (by volume) bound water in the cytoplasmic and extracellular membrane regions would affect the induced E-fields and SARs in cells exposed to 27 or 2450 MHz RF radiation.

A comparison of the results summarized in Table 7 for the seven-component model to the results of Table 3 for the five-component model shows that the inclusion of bound water in these membrane regions had a minimal effect on either the induced E-fields or SARs at either RF frequency. Compared to the membrane-induced SARs in the five-component model, which were 0 at either frequency (because the membrane conductivity was assumed to be zero), the inclusion of water in the membrane caused a slight increase in membrane SAR (0.16 and 0.39 W/kg at 27 and 2450 MHz, respectively) in the water-containing regions of the membrane. To a first approximation, the SARs induced in the bound-water regions in contact with the membrane or within the membrane scaled according to the bound-water volume percentage. Thus, increasing the bound-water volume fraction in the membrane, per se, would result in an increase in SAR in those regions. Available data does not justify such modification of the model at this time.

The implication of these results is that frequency-dependent nonuniformities occur in the distribution of induced E-fields and SARs of the cellular level. Relative to lower RF frequencies (e.g., 27 MHz), the inclusion of a layer of bound water at plasma membrane surfaces resulted in a significant (~60-fold) enhancement in localized SAR in the cell model exposed to 2450 MHz electromagnetic radiation. If, instead of the nominal 1 V/m incident E-field used in these calculations, it is assumed that the incident E-field has a magnitude equal to the ANSI C95.1 [1992] guideline value of 174 V/m (and, for the sake of simplicity, ignoring the alteration in E-field strength due to coupling of the external field to the cell model environment), then the corresponding maximum estimated SAR in the bound-water layer would be approximately 5.6 W/kg. The magnitude of the bound-water SAR predicted by the model calculations suggests that field-induced localized "hot spots" would occur in bound-water layers in cells exposed to microwave radiation under conditions specified by RF health protection guidelines.

Whereas the model predicted the occurrence of localized elevations in SAR, thermodynamic considerations, which are based on fundamental laws of heat conduction, argue against the occurrence of thermal "hot spots," per se. The rate of heat conduction depends on thermal diffusivity, heat capacity, and the characteristic dimensions of the absorber, which, in this instance, is the 0.5 nm thickness of the bound-water layers. The small magnitude of this characteristic bound-water layer dimension is such that the rate of heat transfer would essentially prevent temperature elevation in the bound-water layers. The thermal time constant (τ) of an absorber having a characteristic length (l) is given by the expression:

$$\tau = \frac{l^2 C}{\kappa} \qquad (5)$$

where C is the volume heat capacity, and κ is the thermal conductivity. Assuming values appropriate for water (i.e., $C = 4.2 \times 10^6$ Ws/m^3 °K, $\kappa = 0.6$ W/m °K) and a characteristic length ($l = 0.5 \times 10^{-9}$m), τ of a bound-water layer would be approximately 2×10^{-12} s. Because τ is

at least two orders of magnitude shorter than the period of the maximum RF frequency considered here (2450 MHz), localized RF absorption could not cause differential temperature elevation in a bound-water layer. Thus, whereas the model predicted localized regions of enhanced microwave energy absorption due to coupling to bound water at membrane surfaces, this does not indicate the occurrence of nonuniform heating at the cellular level.

The physiological significance of an enhancement in localized microwave energy density in cell membrane-associated bound water is undetermined. This is due, in part, to limited information on the role of bound water in cell physiological processes. Although the physiological significance of nonuniform electromagnetic energy absorption at the cellular level cannot be ascertained from the results presented here, this approach may provide insight regarding such questions. Future studies will be directed toward determining the role of nonuniform RF energy absorption at the cellular level. In addition, efforts will focus on determining the spatial distribution of RF-induced nonuniform E-field and SAR distributions on the cell surface using the methods described herein.

ACKNOWLEDGMENTS

This work was supported by NIH grants RO1-ES05417 and RO1-OHO2148.

REFERENCES

Cleary SF (1990a): Biological effects of radiofrequency electromagnetic fields. In Gandhi OP (ed): "Biological Effects and Medical Applications of Electromagnetic Energy." Englewood Cliffs, NJ: Prentice Hall, pp 236–255.

Cleary SF (1990b): Cellular effects of radiofrequency electromagnetic fields. In Gandhi OP (ed): "Biological Effects and Medical Applications of Electromagnetic Energy." Englewood Cliffs, NJ: Prentice Hall, pp 339–356.

Cleary SF, Liu LM, Merchant RE (1990a): Lymphocyte proliferation induced by radiofrequency radiation under isothermal conditions. Bioelectromagnetics 11:47–56.

Cleary SF, Liu LM, Merchant RE (1990b): Glioma proliferation modulated in vitro by isothermal radiofrequency radiation exposure. Radiat Res 121:38–45.

Cleary SF, Liu LM, Cao G (1992): Effects of RF power absorption in mammalian cells. In Magin RL, Liburdy RP, Persson P (eds): "Biological Effects and Safety Aspects of Nuclear Magnetic Resonance Imaging and Spectroscopy." Ann NY Acad Sci 649:166–175.

Colonomos P, Gordon RG (1979): Bounded error analysis of experimental distributions of relaxation times. J Chem Phys 71:1159–1166.

Cook R, Kuntz ID (1974): The properties of water in biological systems. Annu Rev Biophys Bioeng 3:95–126.

Dawkins AWJ, Nightingale NRV, South GP, Sheppard RJ, Grant EH (1979): The role of water in microwave absorption by biological material with particular reference to microwave hazards. Physiol Med Biol 24:1168–1179.

Drago GP, Ridella S (1982): Evaluation of electrical fields inside a biological structure. Br J Cancer (Suppl V) 45:215–219.

Foster KR, Chuver E, Leonard JB (1984): Transport properties of polymer solutions: A comparative approach. Biophys J 45:975–984.

Grant EH, Mitton BGR, South GP, Sheppard RJ (1974): An investigation by dielectric methods of hydration in myoglobin solutions. Biochem J 139:375.

Grant EH, Sheppard RJ, South GP (1978): "Dielectric Behavior of Biological Molecules in Solution." Oxford: Clarendon Press, pp 160–165.

Griffith OH, Dehlinger PJ, Van SP (1974): Shape of hydrophobic barrier of phospholipid bilayers (evidence for H_2O penetration in biological membranes). J Membrane Biol 15:159–162.

Jaroszyński W, Terlecki J, Myśliwski A, Myśliwski J, Watkowski J (1983): Dielectric properties of murine lymphocytes. Fol Histochem Cytochem 21:161–1721.

McIntosh TJ, Simon SA, Dilger JP (1989): Location of water-hydrocarbon interface in lipid bilayers. In Benga G (ed): "Water Transport in Biological Membranes, Vol 1." Boca Raton, FL: CRC Press, pp 1–16.

Schwan HP (1971): Interaction of microwave and radio frequency radiation with biological systems. IEEE Trans Microwave Theor Techniques MTT 19:146–152.

Schwan HP (1977): Field interaction with biological matter. Ann NY Acad Sci 303:198–213.

Stratton J (1941): "Electromagnetic Theory." New York: McGraw-Hill, pp 513–573.

Van Bladel J (1985): "Electromagnetic Fields." New York: Hemisphere Publishing Co.